

1                   **An *Escherichia coli* nitrogen starvation response is important**  
2                   **for mutualistic coexistence with *Rhodospseudomonas palustris***

3       Alexandra L. McCully<sup>1</sup>, Megan G. Behringer<sup>2</sup>, Jennifer R. Gliessman<sup>1</sup>, Evgeny V. Pilipenko<sup>3</sup> Jeffrey L.  
4                   Mazny<sup>1</sup>, Michael Lynch<sup>2</sup>, D. Allan Drummond<sup>3</sup>, James B. McKinlay<sup>1#</sup>

5  
6                   <sup>1</sup>Department of Biology, Indiana University, Bloomington, IN

7       <sup>2</sup>School of Life Sciences; Biodesign Center for Mechanisms of Evolution, Arizona State University,  
8                   Tempe, AZ.

9       <sup>3</sup>Department of Biochemistry & Molecular Biology; Department of Human Genetics, University of  
10                   Chicago, Chicago IL.

11  
12  
13       Running title (54 max): Nitrogen starvation response in a bacterial mutualism

14       #Corresponding author. 1001 E 3<sup>rd</sup> Street, Jordan Hall, Bloomington, IN 47405

15       Phone: 812-855-0359

16       Email: jmckinla@indiana.edu

17       **Conflict of interest.**

18       The authors declare no conflict of interest

19 **Abstract (250)**

20 Microbial mutualistic cross-feeding interactions are ubiquitous and can drive important community  
21 functions. Engaging in cross-feeding undoubtedly affects the physiology and metabolism of individual  
22 species involved. However, the nature in which an individual's physiology is influenced by cross-feeding  
23 and the importance of those physiological changes for the mutualism have received little attention. We  
24 previously developed a genetically tractable coculture to study bacterial mutualisms. The coculture  
25 consists of fermentative *Escherichia coli* and phototrophic *Rhodospseudomonas palustris*. In this  
26 coculture, *E. coli* anaerobically ferments sugars into excreted organic acids as a carbon source for *R.*  
27 *palustris*. In return, a genetically-engineered *R. palustris* constitutively converts  $N_2$  into  $NH_4^+$ , providing  
28 *E. coli* with essential nitrogen. Using RNA-seq and proteomics, we identified transcript and protein levels  
29 that differ in each partner when grown in coculture versus monoculture. When in coculture with *R.*  
30 *palustris*, *E. coli* gene expression changes resembled a nitrogen starvation response under the control of  
31 the transcriptional regulator NtrC. By genetically disrupting *E. coli* NtrC, we determined that a nitrogen  
32 starvation response is important for a stable coexistence, especially at low *R. palustris*  $NH_4^+$  excretion  
33 levels. Destabilization of the nitrogen starvation regulatory network resulted in population heterogeneity  
34 and in some cases, extinction. Our results highlight that alternative physiological states can be important  
35 for survival within cooperative cross-feeding relationships.

36

37 **Importance (150)**

38 Mutualistic cross-feeding between microbes within multispecies communities is widespread. Studying  
39 how mutualistic interactions influence the physiology of each species involved is important for  
40 understanding how mutualisms function and persist in both natural and applied settings. Using a bacterial  
41 mutualism consisting of *Rhodospseudomonas palustris* and *Escherichia coli* growing cooperatively  
42 through bidirectional nutrient exchange, we determined that an *E. coli* nitrogen starvation response is  
43 important for maintaining a stable coexistence. The lack of an *E. coli* nitrogen starvation response  
44 ultimately destabilized the mutualism and, in some cases, led to community collapse after serial transfers.

45 Our findings thus inform on the potential necessity of an alternative physiological state for mutualistic  
46 coexistence with another species compared to the physiology of species grown in isolation.

47

## 48 **Introduction**

49 Within diverse microbial communities, species engage in nutrient cross-feeding with reciprocating  
50 partners as a survival strategy (1). In cases where species are not obligate mutualists, transitioning from a  
51 free-living lifestyle to one based on cross-feeding can change the physiological state of the cells involved,  
52 the extent to which depends on the nature of the cross-feeding relationship. For example, cross-feeding  
53 can promote physiological changes that increase virulence (2, 3) or drastically alter cellular metabolism  
54 (4), in some cases allowing for lifestyles that are only possible during mutualistic growth with a partner  
55 (4–7). Aside from these examples, relatively little is known about how cell physiology is influenced by  
56 mutualistic cross-feeding, despite the prevalence of cross-feeding in microbial communities.

57 Synthetic communities, or cocultures, are ideally suited for studying the physiological responses  
58 to cooperative cross-feeding given their tractability (8, 9). We previously developed a bacterial coculture  
59 that consists of fermentative *Escherichia coli* and the N<sub>2</sub>-fixing photoheterotroph *Rhodospseudomonas*  
60 *palustris* (Fig. 1) (10). In this coculture, *E. coli* anaerobically ferments glucose into organic acids,  
61 providing *R. palustris* with essential carbon. In return, a genetically engineered *R. palustris* strain (Nx)  
62 constitutively fixes N<sub>2</sub> gas, resulting in NH<sub>4</sub><sup>+</sup> excretion that provides *E. coli* with essential nitrogen. The  
63 result is an obligate mutualism that maintains a stable coexistence and reproducible growth trends (10) as  
64 long as bidirectional nutrient cross-feeding levels are maintained within a defined range (11, 12).

65 Here we determined how nutrient cross-feeding between *E. coli* and *R. palustris* Nx alters the  
66 physiological state of each partner population. Using RNA-seq and proteomic analyses, we identified  
67 genes in both species that were differentially expressed in coculture compared to monoculture, with *E.*  
68 *coli* exhibiting more overall changes in gene expression than *R. palustris* Nx. Specifically, *E. coli* gene  
69 expression patterns resembled that of nitrogen-deprived cells, as many upregulated genes were within the  
70 nitrogen starvation response regulon, controlled by the master transcriptional regulator NtrC. Genetic

71 disruption of *E. coli ntrC* resulted in variable growth trends at low *R. palustris*  $\text{NH}_4^+$  excretion levels and  
72 prevented long-term mutualistic coexistence with *R. palustris* across serial transfers. Our results highlight  
73 the fact that cross-feeding relationships can stimulate alternative physiological states for at least one of  
74 the partners involved and that adjusting cell physiology to these alternative states can be critical for  
75 maintaining coexistence.

76

## 77 **Results**

78 **Engaging in an obligate mutualism alters the physiology of cooperating partners.** In our coculture, *E.*  
79 *coli* and *R. palustris* Nx carry out complementary anaerobic metabolic processes whose products serve as  
80 essential nutrients for the respective partner. Specifically, *E. coli* ferments glucose into acetate, lactate,  
81 and succinate, which serve as carbon sources for *R. palustris* Nx, while other fermentation products such  
82 as formate and ethanol accumulate; in return *R. palustris* Nx fixes  $\text{N}_2$  and excretes  $\text{NH}_4^+$  as the nitrogen  
83 source for *E. coli* (Fig. 1). We previously demonstrated that our coculture supports a stable coexistence  
84 and exhibits reproducible growth and metabolic trends when started from a wide range of starting species  
85 ratios, including single colonies (10). However, we hypothesized that coculture conditions affected the  
86 physiology of each species, particularly *E. coli*, based on the following observations. First, as growth is  
87 coupled in our coculture, *E. coli* is forced to grow 4.6-times slower in coculture with *R. palustris* Nx than  
88 it does in monoculture with abundant  $\text{NH}_4^+$ , and its growth is restrained to only 10% of the population  
89 (10). In contrast, *R. palustris* Nx grows at a rate in coculture that is comparable to that in monoculture  
90 (12), consuming a mixed pool of excreted organic acids from *E. coli*. Second, coculturing pulls *E. coli*  
91 fermentation forward due to removal of inhibitory end products. Indeed, we observed higher yields of  
92 formate, an *E. coli* fermentation product that *R. palustris* does not consume, in cocultures compared to *E.*  
93 *coli* monocultures (10).

94 To determine changes in gene expression patterns imposed by coculturing, we performed RNA-  
95 seq and comparative proteomic analyses (13) on exponential phase cocultures and monocultures of *E. coli*  
96 and *R. palustris* Nx. To make direct comparisons, all cultures were grown in the same basal anaerobic

97 minimal medium and monocultures were supplemented with the required carbon or nitrogen sources to  
98 permit growth for each species. Cocultures and *E. coli* monocultures were provided glucose as a sole  
99 carbon source, whereas a mixture of organic acids and bicarbonate was provided to *R. palustris* Nx  
100 monocultures, as *R. palustris* does not consume glucose. For a nitrogen source, all cultures were grown  
101 under a N<sub>2</sub> headspace, and *E. coli* monocultures were further supplemented with NH<sub>4</sub>Cl, as *E. coli* is  
102 incapable of using N<sub>2</sub>. We identified several differentially expressed genes between monoculture and  
103 coculture conditions in both species with more differences observed in *E. coli* compared to *R. palustris*  
104 Nx, in agreement with our initial hypothesis (Fig. 2). For *E. coli*, out of 4377 ORFs, 55 were upregulated  
105 and 68 were downregulated (Table 1) (log<sub>2</sub> value cutoff=2). Out of 4836 ORFs in *R. palustris* Nx, 14  
106 were upregulated and 20 were downregulated (Table 1) (log<sub>2</sub> value cutoff=2). We also considered that  
107 due to lower *E. coli* abundance in coculture, the apparently larger *E. coli* gene response may be partly due  
108 to decreased resolution and thus increased error variance. Reassuringly, many of the genes identified as  
109 being differentially expressed by RNA-seq were in agreement with the proteomic results (Table 2). Both  
110 RNA-seq and proteomic analyses identified the *E. coli* ammonium transporter AmtB as an important,  
111 upregulated gene in coculture, corroborating our previous findings that *E. coli* AmtB activity is important  
112 for stable coexistence with *R. palustris* (12). Many *E. coli* genes involved in amino acid and purine  
113 biosynthesis were downregulated in coculture (Table 1, Table 2), consistent with the lower observed  
114 growth rate. Additionally, many *E. coli* flagellar and chemotaxis proteins were downregulated in  
115 coculture (Table 1, Table 2), perhaps suggesting that motility is not important for coculture growth.  
116 Alternatively, lower flagellar and chemotaxis transcript levels could be part of a general stress response  
117 (14), perhaps associated with nitrogen limitation in cocultures. Whereas many of the differentially  
118 expressed *E. coli* genes have been characterized in the literature, the *R. palustris* genes showing the  
119 largest differential expression were uncharacterized genes encoding upregulated putative  
120 alcohol/aldehyde dehydrogenases and a downregulated putative TonB-dependent receptor/siderophore  
121 (Table 1, Table 2). Together, these datasets provide insight on how engaging in obligate cross-feeding  
122 changes the lifestyle of each partner.

123

124 **An *E. coli* nitrogen starvation response is important for mutualistic growth with *R. palustris*.** We

125 chose to further examine differential gene expression patterns in *E. coli* as its growth rate and

126 fermentation profile are drastically affected by coculturing, whereas the *R. palustris* Nx growth rate is

127 similar to that in monoculture. We identified several *E. coli* genes and proteins that were upregulated in

128 coculture with *R. palustris* Nx compared to monoculture growth (Table 1, Table 2). We hypothesized that

129 the deletion of highly upregulated *E. coli* genes would negatively affect its growth in coculture. We made

130 deletions in *E. coli* genes that were identified in both RNA-seq and proteome datasets as well as the

131 highest upregulated *E. coli* transcript (*rutA*). We did not examine the effect of deleting *amtB* in this case

132 as we previously determined it to be important for coculture growth (12). These selected *E. coli* genes

133 were all involved in metabolism of alternative nitrogen sources such as D-ala-D-ala dipeptides (*ddpX*,

134 *ddpA*) (15), pyrimidines (*rutA*) (16), amino acids (*argT*) (17), and polyamines (*patA*, *potF*) (18). In

135 monocultures with 15mM NH<sub>4</sub>Cl, there were negligible differences in growth or fermentation profiles

136 between WT *E. coli* or any of the single deletion mutants (Fig. S1). These results are consistent with

137 findings by others, as these genes are only important when scavenging alternative nitrogen sources that

138 are not present in our defined medium. We next tested these *E. coli* mutants in coculture to test if these

139 genes were important when NH<sub>4</sub><sup>+</sup> is slowly cross-fed from *R. palustris* Nx. In all cocultures of *E. coli*

140 mutants paired with *R. palustris* Nx, there were no differences in the coculture growth curves (Fig. 3A) or

141 the final cell densities of each species (Fig. 3B). Additionally, there were no significant differences in the

142 growth rates, growth yields, or product yields from cocultures containing the *E. coli* mutants (Fig. S2).

143 These data suggest that none of these highly expressed *E. coli* genes are solely important for coculture

144 growth. While it is possible that synergistic expression of these genes is important for *E. coli*'s lifestyle in

145 coculture, the actual nitrogen sources accessed by expression of these genes are absent in the defined

146 medium. Thus, unless *E. coli* gains access to alternative nitrogen sources that we are unaware of in

147 coculture with *R. palustris* Nx, synergistic expression of these genes likely provides little to no benefit.

148 Even though individual deletions of the *E. coli* genes showing high expression in coculture had  
149 no effect on coculture trends, we noted that they were all involved in nitrogen scavenging and fell within  
150 the regulon of the transcription factor, NtrC, which controls the nitrogen starvation response (19). During  
151 nitrogen limitation, the sensor kinase NtrB phosphorylates the response regulator NtrC (19).  
152 Phosphorylated NtrC then binds to DNA and activates expression of ~45 genes (20), including those we  
153 tested genetically above and *amtB*, which we previously determined to be important for coculture growth  
154 (12). To examine the importance of the *E. coli* nitrogen starvation response in coculture, we deleted *ntrC*.  
155 We first checked for any general defects of the resulting  $\Delta$ NtrC mutant in monoculture with 15 mM  
156  $\text{NH}_4\text{Cl}$  and found that it exhibited similar growth and metabolic trends to WT *E. coli* (Fig. S3). We then  
157 paired *E. coli*  $\Delta$ NtrC with *R. palustris* Nx in coculture. Compared to cocultures using WT *E. coli*,  
158 cocultures with *E. coli*  $\Delta$ NtrC exhibited slower growth rates, longer lag periods (Fig. 4A), and lower final  
159 *E. coli* cell densities (Fig. 4D). The long lag phase was less prominent in starter cocultures inoculated  
160 from single colonies (Fig. S4A) compared to test cocultures inoculated with a 1% dilution of the starter  
161 cocultures (Fig. 4A). This result suggests that starting *E. coli*  $\Delta$ NtrC cocultures from single colonies  
162 stimulated early growth, perhaps by increasing the *E. coli* frequency to be similar to that of *R. palustris*  
163 when started with colonies of similar sizes rather than a dilution of stationary cocultures wherein the *E.*  
164 *coli* frequency was low (~0.1%; Fig. 4D). A higher initial *E. coli* frequency might help *E. coli* acquire  
165 excreted  $\text{NH}_4^+$  before it is taken back up by *R. palustris* cells and thereby promote reciprocal cross-  
166 feeding, similar to what we observed previously in cocultures with *E. coli*  $\Delta$ AmtB mutants that were  
167 defective for  $\text{NH}_4^+$  uptake (12).

168 The overall coculture metabolism was also altered when *E. coli*  $\Delta$ NtrC was paired with *R.*  
169 *palustris* Nx. In cocultures pairing WT *E. coli* with *R. palustris* Nx, glucose is typically fully consumed  
170 within 5 days coinciding with the accumulation of formate and ethanol (10). Cocultures pairing *E. coli*  
171  $\Delta$ NtrC with *R. palustris* Nx differed in this regard, leaving ~40% of the glucose unconsumed after 10  
172 days and exhibiting little to no formate and ethanol accumulation (Fig. S4B). Even despite the lower  
173 glucose consumption, the final *R. palustris* cell density of cocultures pairing *R. palustris* Nx with *E. coli*

174  $\Delta$ NtrC was similar to those with WT *E. coli*. This unexpectedly high cell density could be explained by  
175 consumption of formate and ethanol by *R. palustris* Nx, though we have never observed consumption of  
176 formate by *R. palustris* Nx in monoculture. Alternatively, a lack of formate and/or ethanol production by  
177 *E. coli* could explain the high cell density if the fermentation profile were shifted towards organic acids  
178 that *R. palustris* normally consumes, namely acetate, lactate and succinate. Together, these data indicate  
179 that misregulation of the nitrogen starvation response affected coculture growth and metabolism.

180 As noted above, the low *E. coli*  $\Delta$ NtrC population and decreased coculture growth rate when  
181 paired with *R. palustris* Nx resembled trends from cocultures that contained *E. coli*  $\Delta$ AmtB mutants (12).  
182 We previously found that the *E. coli*  $\text{NH}_4^+$  transporter, AmtB, was required for coexistence with *R.*  
183 *palustris* Nx across serial transfers as the transporter gives *E. coli* a competitive advantage in acquiring  
184 the transiently available  $\text{NH}_4^+$  before it can be reclaimed by the *R. palustris* population (12). To determine  
185 if *E. coli*  $\Delta$ NtrC was capable of maintaining a stable coexistence in coculture, we inoculated cocultures of  
186 *E. coli*  $\Delta$ NtrC paired with *R. palustris* Nx at equivalent CFUs and performed serial transfers every 10  
187 days. While average final *E. coli* frequencies were consistently between 0.6 – 2.8 % (Fig. 5A), the values  
188 became variable across serial transfers, as did coculture growth rates, lag periods, and net changes in both  
189 *E. coli* and *R. palustris* cell densities (Fig. 5). This variability was due to 2 of the 4 lineages exhibiting  
190 improved coculture growth over successive transfers (Fig. 5B,C), perhaps due to the emergence of  
191 compensatory mutations, while the other two lineages showed declining growth trends (Fig. 5D,E).  
192 Indeed, by transfers 5 and 6 there was little to no coculture growth in the slower-growing lineages (Fig  
193 4D,E). The heterogeneity in growth trends through of serial transfers of cocultures with *E. coli*  $\Delta$ NtrC is  
194 in stark contrast to the stability of cocultures with WT *E. coli*, which we have serially transferred over 100  
195 times with no extinction events (McKinlay, unpublished data). The nitrogen starvation response thus  
196 appears to be important for long-term survival of the mutualism.

197

198 **Increased  $\text{NH}_4^+$  cross-feeding levels can compensate for the absence of a nitrogen starvation**  
199 **response.** The NtrC regulon is critical during periods of nitrogen starvation, activating a wide variety of



200 genes that are important for scavenging diverse nitrogen sources (20). We hypothesized that higher *R.*  
201 *palustris* NH<sub>4</sub><sup>+</sup> cross-feeding levels could mitigate the poor growth of *E. coli* ΔNtrC in coculture by  
202 making the nitrogen starvation response less important for survival. Previously, we engineered an *R.*  
203 *palustris* Nx strain that excretes 3-times more NH<sub>4</sub><sup>+</sup> by deleting *R. palustris* NH<sub>4</sub><sup>+</sup> transporters encoded by  
204 *amtB1* and *amtB2* (NxΔAmtB) (10). N<sub>2</sub>-fixing bacteria use AmtB to reacquire NH<sub>4</sub><sup>+</sup> that leaks outside the  
205 cell, and ΔAmtB mutants thus accumulate NH<sub>4</sub><sup>+</sup> into the supernatant (10, 12, 21). In agreement with our  
206 hypothesis, cocultures with *R. palustris* NxΔAmtB exhibited similar growth trends regardless of the *E.*  
207 *coli* strain used (Fig. 4B,D). As *R. palustris* NxΔAmtB excretes more NH<sub>4</sub><sup>+</sup> than *R. palustris* Nx, it was  
208 previously shown to result in faster WT *E. coli* growth and subsequent fermentation rates in coculture,  
209 ultimately leading to the accumulation of consumable organic acids (Fig. S4B) and acidification of the  
210 medium, inhibiting *R. palustris* growth (10). Cocultures pairing *R. palustris* NxΔAmtB and *E. coli* ΔNtrC  
211 similarly exhibited growth (Fig. 4B,D), and fermentation profile trends (Fig. S4B) that were  
212 indistinguishable from cocultures pairing *R. palustris* NxΔAmtB with WT *E. coli*. These similar trends  
213 indicate that high *R. palustris* NH<sub>4</sub><sup>+</sup> excretion can eliminate the trends observed when the *E. coli* nitrogen  
214 starvation response is compromised due to a ΔNtrC mutation.

215 One possibility for why high NH<sub>4</sub><sup>+</sup> cross-feeding levels eliminate the need for *E. coli* *ntrC* is that  
216 the free NH<sub>4</sub><sup>+</sup> levels might be sufficiently high enough to prevent activation of the *E. coli* NtrC regulon.  
217 However, comparative RNA-seq and proteomic analyses revealed that the same *E. coli* genes within the  
218 NtrC regulon that were highly upregulated in cocultures pairing WT *E. coli* with *R. palustris* Nx were  
219 also upregulated in cocultures with *R. palustris* NxΔAmtB (Table 1, Table 2). Thus, even though the *E.*  
220 *coli* nitrogen starvation response is activated when cocultured with *R. palustris* NxΔAmtB, this response  
221 is likely dispensable if there is sufficiently high NH<sub>4</sub><sup>+</sup> cross-feeding.

222

223 ***E. coli* NtrC is required for adequate AmtB expression to access cross-fed NH<sub>4</sub><sup>+</sup> in coculture.** While  
224 a high level of *R. palustris* NH<sub>4</sub><sup>+</sup> excretion can compensate for an improper *E. coli* nitrogen starvation  
225 response, less NH<sub>4</sub><sup>+</sup> excretion could potentially exaggerate problems emerging from the absence of NtrC.

226 We previously constructed an *R. palustris*  $\Delta$ AmtB strain that excreted 1/3<sup>rd</sup> of the  $\text{NH}_4^+$  than *R. palustris*  
227 Nx in monoculture and which could not coexist in coculture with *R. palustris*  $\Delta$ AmtB (12). The reason for  
228 this lack of coexistence was due to *R. palustris*  $\Delta$ AmtB outcompeting *E. coli*  $\Delta$ AmtB for the lower level  
229 of transiently available  $\text{NH}_4^+$ , thus limiting *E. coli* growth and thereby the reciprocal supply of  
230 fermentation products to *R. palustris* (12). Expression of *E. coli* *amtB* is thus important in coculture in  
231 order to maintain coexistence. Indeed, RNA-seq and proteomic analyses revealed that *E. coli* AmtB  
232 transcript and protein levels were upregulated in all cocultures pairing WT *E. coli* with any of the three *R.*  
233 *palustris* strains (Nx, Nx $\Delta$ AmtB,  $\Delta$ AmtB) (Table 1, Table 2). We thus wondered whether *E. coli*  $\Delta$ NtrC  
234 would coexist with the low  $\text{NH}_4^+$ -excreting strain *R. palustris*  $\Delta$ AmtB in coculture, as *E. coli* *amtB*  
235 expression is transcriptionally activated by NtrC. Consistent with our previous findings, *R. palustris*  
236  $\Delta$ AmtB supported a high relative WT *E. coli* population in coculture (Fig. 4D) (12). When cocultured  
237 with WT *E. coli*, *R. palustris*  $\Delta$ AmtB responds to  $\text{NH}_4^+$  loss to *E. coli* by upregulating nitrogenase activity  
238 since it has a wild-type copy of NifA (12). As a result, *R. palustris*  $\Delta$ AmtB cross-feeds enough  $\text{NH}_4^+$  to  
239 stimulate a high WT *E. coli* frequency and subsequent accumulation of consumable organic acids, similar  
240 to cocultures with *R. palustris* Nx $\Delta$ AmtB (Fig 3D, Fig. S4B) (12). In contrast, when we paired *E. coli*  
241  $\Delta$ NtrC with *R. palustris*  $\Delta$ AmtB, little to no coculture growth was observed (Fig. 4C), similar to previous  
242 observations in cocultures pairing *E. coli*  $\Delta$ AmtB with *R. palustris*  $\Delta$ AmtB (12). Starter cocultures  
243 inoculated with single colonies of each species in this pairing grew to low cell densities (Fig. S4A), and  
244 test cocultures inoculated from these starter cocultures resulted in little to no growth, even after prolonged  
245 incubation (Fig. 4C).

246 As AmtB is under the control of NtrC (20), we hypothesized that cocultures pairing *E. coli*  $\Delta$ NtrC  
247 with *R. palustris*  $\Delta$ AmtB resulted in insufficient *E. coli* *amtB* expression, leading to poor competition for  
248  $\text{NH}_4^+$ , which *R. palustris* will require if given the chance (12). We thus predicted that increased  
249 expression of *amtB* in *E. coli*  $\Delta$ NtrC would result in increased net growth of both species, as *E. coli*  
250  $\Delta$ NtrC would be more competitive for essential  $\text{NH}_4^+$  and be able to grow and produce more organic acids

251 for *R. palustris*  $\Delta$ AmtB. To test this prediction, we obtained a plasmid harboring an IPTG-inducible copy  
252 of *amtB* (*pamtB*) for use in *E. coli*  $\Delta$ NtrC. AmtB is typically tightly regulated and only expressed when  
253  $\text{NH}_4^+$  concentrations are below 20  $\mu\text{M}$ , as cells acquire sufficient  $\text{NH}_4^+$  through passive diffusion of  $\text{NH}_3$   
254 across the membrane at higher concentrations (22). Additionally, excessive  $\text{NH}_4^+$  uptake through AmtB  
255 transporters that exceeds the rate of assimilation can result in a futile cycle, as excess  $\text{NH}_3$  inevitably  
256 diffuses outside the cell (19). We first tested the effect of *pamtB* in WT *E. coli* monocultures with 15 mM  
257  $\text{NH}_4\text{Cl}$ . Induction with 1 mM IPTG prevented growth whereas 0.1 mM IPTG permitted growth albeit at a  
258 decreased growth rate (Fig. S5). We thus decided to use 0.1 mM IPTG to induce *amtB* expression in all  
259 cocultures described below. In cocultures pairing *E. coli*  $\Delta$ NtrC *pamtB* with *R. palustris*  $\Delta$ AmtB, more  
260 growth was observed than in cocultures with *E. coli*  $\Delta$ NtrC harboring an empty vector (pEV) (Fig. 6A). In  
261 cocultures with *E. coli*  $\Delta$ NtrC pEV, the *R. palustris*  $\Delta$ AmtB cell density increased whereas the *E. coli* cell  
262 density did not (Fig. 6B). The *R. palustris* growth was likely due to growth-independent cross-feeding of  
263 fermentation products from *E. coli* maintenance metabolism, a phenomenon we described previously  
264 (11). In contrast, cell densities of both species increased in cocultures pairing *R. palustris*  $\Delta$ AmtB with *E.*  
265 *coli*  $\Delta$ NtrC *pamtB* (Fig. 6C), in agreement with our hypothesis that poor *E. coli* *amtB* expression  
266 contributed to the lack of growth in this coculture pairing. Thus, while we cannot rule out that other genes  
267 within the *E. coli* *ntrC* regulon are not important for coculture growth, the necessity of NtrC to upregulate  
268 *amtB* is clearly important.

269

## 270 **Discussion**

271 In this study, we found that reciprocal nutrient cross-feeding between *E. coli* and *R. palustris* resulted in  
272 significant changes in gene expression in both species compared to monocultures. Based on the RNA-seq  
273 and proteomic analyses, we determined that *E. coli* alters its physiology to adopt a nitrogen-starved state  
274 in response to low  $\text{NH}_4^+$  cross-feeding levels from *R. palustris*. We subsequently determined that this  
275 nitrogen-starved state is important for coexistence as genetic elimination of the master transcriptional  
276 regulator, NtrC, resulted in variable population outcomes. Mutualistic nutrient cross-feeding has also been

277 shown to change the lifestyle of interacting partners in other systems. In natural communities, nutrient  
278 cross-feeding can alter gene expression patterns to adapt each species to a syntrophic lifestyle (23–26). In  
279 some cases, the lifestyles exhibited within a mutualism might not even be possible during growth in  
280 isolation. For example, in synthetic communities that pair the sulfate-reducer *Desulfovibrio vulgaris* with  
281 the methanogen *Methanococcus maripaludis*, the methanogen consumes H<sub>2</sub> to maintain low partial  
282 pressures that permit the sulfate reducer to adopt a fermentative lifestyle that would otherwise be  
283 thermodynamically infeasible (5). Similarly, in an experimental *Geobacter* coculture, direct electron  
284 transfer from *Geobacter metallireducens* to *Geobacter sulfurreducens* makes ethanol fermentation by *G.*  
285 *metallireducens* thermodynamically possible (7).

286         Similar to our mutualistic system, the mutualism between *D. vulgaris* and *M. maripaludis*  
287 represents a facultative mutualism, at least in the short term prior to evolutionary erosion of independent  
288 lifestyles (27). For mutualistic relationships to persist between partners that are conditionally capable of a  
289 free-living lifestyle, the relationship must exhibit resilience, or the ability to recover its function after a  
290 disturbance (28). One important resilience factor is the activation of regulatory networks that allow for  
291 microbes to quickly respond to environmental perturbations. Whereas flexible gene expression is useful  
292 for an individual microbe's survival, excessive flexibility can sometimes lead to community collapse  
293 between mutualists in a fluctuating environment (29, 30). In the aforementioned coculture of *D. vulgaris*  
294 and *M. maripaludis*, it was shown that alternating between coculture and monoculture conditions, which  
295 require different metabolic lifestyles, resulted in community collapse (29, 30). Surprisingly, community  
296 collapse could be avoided by mutations that disrupted the *D. vulgaris* regulatory response needed to adapt  
297 cells for optimal growth rates in monoculture (29). Disruption of this regulatory response resulted in a  
298 heterogeneous *D. vulgaris* population, ensuring that a subpopulation would be primed for immediate  
299 mutualistic growth upon transition between growth conditions (30). In our system, the *E. coli* nitrogen  
300 starvation regulatory network was specifically activated by coculturing with *R. palustris* and was  
301 important for coculture stability. It is currently unclear if transitioning *E. coli* between monoculture and

302 coculture conditions would result in similar community collapse or whether the NtrC-regulated network  
303 would adjust rapidly enough to meet the demands of each condition.

304 Nutrient starvation and other stress responses are widely conserved in diverse microbes and are  
305 primarily regarded as necessary for an individual's survival in nutrient-limited environments (31–34).  
306 Many microbial communities are composed of primarily slow-growing or even non-growing  
307 subpopulations (35–37). However, lack of microbial growth in these communities does not imply  
308 cessation of cross-feeding, as bacteria often carry out growth-independent maintenance processes at slow  
309 rates (38), and such activities can be coupled to cross-feeding (11). Our findings suggest that nutrient  
310 starvation and perhaps other stress responses can help stabilize microbial cross-feeding interactions,  
311 especially at low nutrient cross-feeding levels. The extent to which specific starvation or stress responses  
312 are active in diverse mutualistic relationships remains unclear, yet likely depends on the environmental  
313 context. Together our results highlight the important role that alternate physiological states, including  
314 stress responses, can play in establishing and maintaining mutualistic cross-feeding relationships.

315

## 316 **Materials and Methods**

317 **Strains and growth conditions.** Strains, plasmids, and primers are listed in Table S1. All *R. palustris*  
318 strains contained  $\Delta uppE$  and  $\Delta hupS$  mutations to facilitate accurate colony forming unit (CFU)  
319 measurements by preventing cell aggregation (39) and to prevent H<sub>2</sub> uptake, respectively. *E. coli* was  
320 cultivated on Luria-Burtani (LB) agar and *R. palustris* on defined mineral (PM) (40) agar with 10 mM  
321 succinate. (NH<sub>4</sub>)<sub>2</sub>SO<sub>4</sub> was omitted from PM agar for determining *R. palustris* CFUs. Monocultures and  
322 cocultures were grown in 10 mL of defined M9-derived coculture medium (MDC) (10) in 27-mL  
323 anaerobic test tubes under 100% N<sub>2</sub> as described (10). MDC was supplemented with cation solution (1 %  
324 v/v; 100 mM MgSO<sub>4</sub> and 10 mM CaCl<sub>2</sub>) and glucose (25 mM), unless indicated otherwise. All cultures  
325 were grown at 30°C laying horizontally under a 60 W incandescent bulb with shaking at 150 rpm. Starter  
326 cocultures were inoculated with 200 μL MDC containing a suspension of a single colony of each species.  
327 Test cocultures and serial transfers were inoculated using a 1% dilution from starter cocultures. For

328 experiments requiring a starting species ratio of 1:1, *E. coli* and *R. palustris* starter monocultures were  
329 grown to equivalent cell densities, and inoculated at equal volumes. For harvesting RNA and protein, 100  
330 mL cultures were grown shaking in 260-mL serum vials with 25 mM glucose and 10 mM cation solution.  
331 *R. palustris* monocultures were further supplemented with 15 mM sodium bicarbonate and an organic  
332 acid mixture containing 7.8 mM sodium acetate, 8.7 mM disodium succinate, 1.5 mM sodium lactate, 0.3  
333 mM sodium formate, and 6.7mM ethanol as carbon sources. *E. coli* monocultures were supplemented  
334 with 2.5 mM NH<sub>4</sub>Cl as a nitrogen source. Kanamycin was added to a final concentration of 30 µg/ml for  
335 *E. coli* where appropriate. Chloramphenicol was added to a final concentration of 5 µg/ml for both *R.*  
336 *palustris* and *E. coli* where appropriate.

337 **Generation of *E. coli* mutants.** P1 transduction (41) was used to introduce deletions from Keio  
338 collection strains into MG1655. The genotype of kanamycin-resistant colonies was confirmed by PCR  
339 and sequencing.

340 **Analytical procedures.** Cell density was assayed by optical density at 660 nm (OD<sub>660</sub>) using a Genesys  
341 20 visible spectrophotometer (Thermo-Fisher, Waltham, MA, USA). Growth curve readings were taken  
342 in culture tubes without sampling (i.e., tube OD<sub>660</sub>). Specific growth rates were determined using readings  
343 between 0.1-1.0 OD<sub>660</sub> where there is linear correlation between cell density and OD<sub>660</sub>. Final OD<sub>660</sub>  
344 measurements were taken in cuvettes and samples were diluted into the linear range as necessary.  
345 Glucose, organic acids, formate and ethanol were quantified using a Shimadzu high-performance liquid  
346 chromatograph (HPLC) as described (42).

347 **Sample collection for transcriptomics and proteomics.** Monocultures and cocultures were grown in  
348 100-mL volumes to late exponential phase and immediately chilled in an ice-water bath. A 1-mL sample  
349 was collected for protein quantification using a Pierce BCA Protein Assay Kit as per the manufacturer's  
350 protocol. A 5-ml sample was removed for RNA extraction and 90 ml was used for proteomic analysis. All  
351 samples were centrifuged at 4°C to pellet cells, frozen in liquid N<sub>2</sub>, and stored at -80°C until processing.

352 **RNA-seq.** Total RNA was isolated from late exponential cell pellets using the RNeasy kit (Qiagen,  
353 Valencia, CA, USA) as per the manufacturer's protocol. In order to calculate baseline expression levels,

354 RNA sequencing reads resulting from monoculture were mapped to their corresponding reference genome  
355 (*E. coli* str. K-12 substr. MG1655 (43), NCBI RefSeq: NC\_000913.3; *R. palustris* CGA0009 (44), NCBI  
356 RefSeq: NC\_005296.1) using the Tuxedo protocol for RNA expression analysis (45) (Workflow  
357 deposited at <https://github.com/behring/Task3/RNASeq>). Specifically, split-reads were aligned to the  
358 reference genome with Tophat2 (v.2.1.0) (46) and Bowtie2 (v.2.1.0) (47). Following mapping, transcripts  
359 were assembled with cufflinks (v.2.2.0) (48), and differential expression was identified with the cufflinks  
360 tool, cuffdiff (v.2.2.0). To assure that crossmapping of homologous sequencing reads would not  
361 complicate expression analysis from the co-culture experiments, monoculture reads were additionally  
362 mapped as described to the opposing genome. As all potential crossmapping was confined to residual  
363 rRNA reads, these regions were excluded from the analysis and the co-culture RNA-seq reads were  
364 analyzed by mapping the sequenced reads to both reference genomes with no further correction.

365 **Analysis by LC-MS/MS.** Mass spectrometry was performed at the Mass Spectrometry and Proteomics  
366 Research Laboratory (MSPRL), FAS Division of Science, at Harvard University. Samples were  
367 individually labeled with tandem mass tag (TMT) 10-plex reagents according to the manufacturer's  
368 protocol (ThermoFisher Scientific) and mixed. The mixed sample was dried in a speedvac and re-diluted  
369 with Buffer A (0.1 % formic acid in water) for injection for HPLC runs. The sample was submitted for a  
370 single liquid chromatography coupled to tandem mass spectrometry (LC-MS/MS) experiment which was  
371 performed on a LTQ Orbitrap Elite (ThermoFisher Scientific) equipped with Waters (Milford, MA)  
372 NanoAcquity HPLC pump. Peptides were separated onto a 100  $\mu\text{m}$  inner diameter microcapillary trapping  
373 column packed first with approximately 5 cm of C18 Reprosil resin (5  $\mu\text{m}$ , 100  $\text{\AA}$ , Dr. Maisch GmbH,  
374 Germany) followed by analytical column ~20 cm of Reprosil resin (1.8  $\mu\text{m}$ , 200  $\text{\AA}$ , Dr. Maisch GmbH,  
375 Germany). Separation was achieved through applying a gradient from 5–27% ACN in 0.1% formic acid  
376 over 90 min at 200  $\text{nl min}^{-1}$ . Electrospray ionization was enabled through applying a voltage of 1.8 kV  
377 using a home-made electrode junction at the end of the microcapillary column and sprayed from fused  
378 silica pico tips (New Objective, MA). The LTQ Orbitrap Elite was operated in data-dependent mode for  
379 the mass spectrometry methods. The mass spectrometry survey scan was performed in the Orbitrap in the

380 range of 395 –1,800 m/z at a resolution of  $6 \times 10^4$ , followed by the selection of the twenty most intense  
381 ions (TOP20) for CID-MS2 fragmentation in the ion trap using a precursor isolation width window of 2  
382 m/z, AGC setting of 10,000, and a maximum ion accumulation of 200 ms. Singly charged ion species  
383 were not subjected to CID fragmentation. Normalized collision energy was set to 35 V and an activation  
384 time of 10 ms. Ions in a 10 ppm m/z window around ions selected for MS2 were excluded from further  
385 selection for fragmentation for 60 s. The same TOP20 ions were subjected to HCD MS2 event in Orbitrap  
386 part of the instrument. The fragment ion isolation width was set to 0.7 m/z, AGC was set to 50,000, the  
387 maximum ion time was 200 ms, normalized collision energy was set to 27V and an activation time of 1  
388 ms for each HCD MS2 scan.

389 **Mass spectrometry data analysis.** Raw data were submitted for analysis in MaxQuant 1.5.6.5 (13).  
390 Assignment of MS/MS spectra was performed by searching the data against a protein sequence database  
391 including all entries from the *E. coli* MG1655 proteome (49), the *R. palustris* CGA009 proteome (44),  
392 and other known contaminants such as human keratins and common lab contaminants. MaxQuant  
393 searches were performed using a 20 ppm precursor ion tolerance with a requirement that each peptide had  
394 N termini consistent with trypsin protease cleavage, allowing up to two missed cleavage sites. 10-plex  
395 TMT tags on peptide amino termini and lysine residues were set as static modifications while methionine  
396 oxidation and deamidation of asparagine and glutamine residues were set as variable modifications. MS2  
397 spectra were assigned with a false discovery rate (FDR) of 1% at the protein level by target-decoy  
398 database search. Per-peptide reporter ion intensities were exported from MaxQuant (evidence.txt). Only  
399 peptides with a parent ion fraction greater than or equal to 0.5 were used for subsequent analysis (6063 of  
400 9987 peptides). Intensities were calculated as the sum of peptide intensities. Ratios between conditions  
401 were computed at the peptide level, and the protein ratio was computed as the mean of peptide ratios. All  
402 ratios were normalized by dividing by the median value for proteins from the same species. Ratio  
403 significance for coculture conditions at an FDR of 1% was computed by determining the ratio  $r$  at which  
404 99% of genes have ratio less than  $r$  when comparing biological replicate monocultures.

405



406 **Expression of *E. coli amtB* in coculture.** The ASKA collection (50) plasmid harboring an IPTG-  
407 inducible copy of *amtB* (pCA24N *amtB*) was purified from strain JW0441-AM and introduced by  
408 electroporation into WT *E. coli* and  $\Delta$ NtrC. Cocultures were inoculated with either single colonies of each  
409 species or at a 1:1 starting species ratio, as indicated in the figure legends. IPTG and 5  $\mu$ g/ml  
410 chloramphenicol were supplemented to cocultures to induce *E. coli amtB* expression in cocultures and  
411 maintain the plasmid, respectively.

412

### 413 **Acknowledgments**

414 We thank B. A. Budnik and R. A. Robins (Harvard MSPRL) for assistance with mass spectrometry.

415 We thank P. L. Foster for providing the Keio and ASKA *E. coli* collections. This work was supported in  
416 part by the U.S. Department of Energy, Office of Science, Office of Biological and Environmental  
417 Research, under Award Number DE-SC0008131, by the U.S. Army Research Office, grant W911NF-14-  
418 1-0411, by a National Institutes of Health National Service Award F32GM123703 to M. G. Behringer,  
419 and by the Indiana University College of Arts and Sciences.

420

### 421 **References**

- 422 1. **Seth EC, Taga ME.** 2014. Nutrient cross-feeding in the microbial world. *Front. Microbiol.* **5**:1–6.
- 423 2. **Hammer ND, Cassat JE, Noto MJ, Lojek LJ, Chadha AD, Schmitz JE, Creech CB, Skaar**  
424 **EP.** 2014. Inter- and Intraspecies Metabolite Exchange Promotes Virulence of Antibiotic-Resistant  
425 *Staphylococcus aureus*. *Cell Host Microbe* **16**:531–537.
- 426 3. **Ramsey MM, Rumbaugh KP, Whiteley M.** 2011. Metabolite cross-feeding enhances virulence  
427 in a model polymicrobial infection. *PLoS Pathog.* **7**:1–8.
- 428 4. **Iannotti EL, Kafkewit D, Wolin MJ, Bryant MP.** 1973. Glucose Fermentation Products of  
429 *Ruminococcus-Albus* Grown in Continuous Culture with *Vibrio-Succinogenes* - Changes Caused  
430 by Interspecies Transfer of H<sub>2</sub>. *J. Bacteriol.* **114**:1231–1240.
- 431 5. **Stolyar S, Van Dien S, Hillesland KL, Pinel N, Lie TJ, Leigh J a, Stahl D a.** 2007. Metabolic

- 432 modeling of a mutualistic microbial community. *Mol. Syst. Biol.* **3**:92.
- 433 6. **Walker CB, Redding-Johanson AM, Baidoo EE, Rajeev L, He Z, Hendrickson EL,**  
434 **Joachimiak MP, Stolyar S, Arkin AP, Leigh J a, Zhou J, Keasling JD, Mukhopadhyay A,**  
435 **Stahl D a.** 2012. Functional responses of methanogenic archaea to syntrophic growth. *ISME J.*  
436 **6**:2045–2055.
- 437 7. **Summers ZM, Fogarty HE, Leang C, Franks AE, Malvankar NS, Lovley DR.** 2010. Direct  
438 exchange of electrons within aggregates of an evolved syntrophic coculture of anaerobic bacteria.  
439 *Science* **330**:1413–5.
- 440 8. **Widder S, Allen RJ, Pfeiffer T, Curtis TP, Wiuf C, Sloan WT, Cordero OX, Brown SP,**  
441 **Momeni B, Shou W, Kettle H, Flint HJ, Haas AF, Laroche B, Kreft J.** 2016. Challenges in  
442 microbial ecology: building predictive understanding of community function and dynamics. *ISME*  
443 *J* **10**:2557–2568.
- 444 9. **Lindemann SR, Bernstein HC, Song H-S, Fredrickson JK, Fields MW, Shou W, Johnson**  
445 **DR, Beliaev AS.** 2016. Engineering microbial consortia for controllable outputs. *ISME J.*  
446 **10**:2077–2084.
- 447 10. **LaSarre B, McCully AL, Lennon JT, McKinlay JB.** 2017. Microbial mutualism dynamics  
448 governed by dose-dependent toxicity of cross-fed nutrients. *ISME J* **11**:337–348.
- 449 11. **McCully AL, LaSarre B, McKinlay JB.** 2017. Growth-independent cross-feeding modifies  
450 boundaries for coexistence in a bacterial mutualism. *Environ. Microbiol.*
- 451 12. **McCully AL, LaSarre B, McKinlay JB.** 2017. Recipient-biased competition for an  
452 intracellularly generated cross-fed nutrient is required for coexistence of microbial mutualists.  
453 *MBio* **8**:e01620-17.
- 454 13. **Cox J, Mann M.** 2008. MaxQuant enables high peptide identification rates, individualized p.p.b.-  
455 range mass accuracies and proteome-wide protein quantification. *Nat. Biotechnol.* **26**:1367–1372.
- 456 14. **Jozefczuk S, Klie S, Catchpole G, Szymanski J, Cuadros-Inostroza A, Steinhauser D, Selbig**  
457 **J, Willmitzer L.** 2010. Metabolomic and transcriptomic stress response of *Escherichia coli*. *Mol.*

- 458 Syst. Biol. **6**:1–16.
- 459 15. **Lessard IAD, Pratt SD, Mccafferty DG, Bussiere DE, Hutchins C, Wanner BL, Katz L,**  
460 **Walsh CT.** 1998. Homologs of the vancomycin resistance D-Ala-D-Ala dipeptidase VanX in  
461 *Streptomyces toyocaensis*, *Escherichia coli* and *Synechocystis* □: attributes of catalytic efficiency  
462, stereoselectivity and regulation with implications for function. *Chem. Biol.* **5**.
- 463 16. **Kim KS, Pelton JG, Inwood WB, Andersen U, Kustu S, Wemmer DE.** 2010. The Rut pathway  
464 for pyrimidine degradation: Novel chemistry and toxicity problems. *J. Bacteriol.* **192**:4089–4102.
- 465 17. **Caldara M, Charlier D, Cunin R.** 2006. The arginine regulon of *Escherichia coli*: Whole-system  
466 transcriptome analysis discovers new genes and provides an integrated view of arginine regulation.  
467 *Microbiology* **152**:3343–3354.
- 468 18. **Kashiwagi K, Pistocchi R, Shibuya S, Sugiyama S, Morikawa K, Igarashi K.** 1996.  
469 Spermidine-preferential Uptake System in *Escherichia coli*. *J. Biol. Chem.* **271**:12205–12208.
- 470 19. **van Heeswijk WC, Westerhoff H V., Boogerd FC.** 2013. Nitrogen Assimilation in *Escherichia*  
471 *coli*: Putting Molecular Data into a Systems Perspective. *Microbiol. Mol. Biol. Rev.* **77**:628–695.
- 472 20. **Zimmer DP, Soupene E, Lee HL, Wendisch VF, Khodursky AB, Peter BJ, Bender RA,**  
473 **Kustu S.** 2000. Nitrogen regulatory protein C-controlled genes of *Escherichia coli*: scavenging as  
474 a defense against nitrogen limitation. *Proc. Natl. Acad. Sci. U. S. A.* **97**:14674–14679.
- 475 21. **Barney BM, Eberhart LJ, Ohlert JM, Knutson CM, Plunkett MH.** 2015. Gene Deletions  
476 Resulting in Increased Nitrogen Release by *Azotobacter vinelandii*: Application of a Novel  
477 Nitrogen Biosensor. *Appl. Environ. Microbiol.* **81**:4316–4328.
- 478 22. **Kim M, Zhang Z, Okano H, Yan D, Groisman A, Hwa T.** 2012. Need-based activation of  
479 ammonium uptake in *Escherichia coli*. *Mol. Syst. Biol.* **8**:1–10.
- 480 23. **Rosenthal AZ, Matson EG, Eldar A, Leadbetter JR.** 2011. RNA-seq reveals cooperative  
481 metabolic interactions between two termite-gut spirochete species in co-culture. *ISME J.* **5**:1133–  
482 1142.
- 483 24. **Filkins LM, Graber J a., Olson DG, Dolben EL, Lynd LR, Bhujju S, Toole AO, O’Toole G a.**

- 484 2015. Coculture of *Staphylococcus aureus* with *Pseudomonas aeruginosa* Drives *S. aureus* towards  
485 Fermentative Metabolism and Reduced Viability in a Cystic Fibrosis Model. *J. Bacteriol.*  
486 **197**:JB.00059-15.
- 487 25. **Men Y, Feil H, VerBerkmoes NC, Shah MB, Johnson DR, Lee PKH, West KA, Zinder SH,**  
488 **Andersen GL, Alvarez-Cohen L.** 2012. Sustainable syntrophic growth of *Dehalococcoides*  
489 *ethenogenes* strain 195 with *Desulfovibrio vulgaris* Hildenborough and *Methanobacterium*  
490 *congolense*: global transcriptomic and proteomic analyses. *ISME J.* **6**:410–421.
- 491 26. **Giannone RJ, Huber H, Karpinets T, Heimerl T, Küper U, Rachel R, Keller M, Hettich RL,**  
492 **Podar M.** 2011. Proteomic characterization of cellular and molecular processes that enable the  
493 *Nanoarchaeum equitans-ignicoccus hospitalis* relationship. *PLoS One* **6**.
- 494 27. **Hillesland KL, Lim S, Flowers JJ, Turkarslan S, Pinel N, Zane GM, Elliott N, Qin Y, Wu L,**  
495 **Baliga NS, Zhou J, Wall JD, Stahl DA.** 2014. Erosion of functional independence early in the  
496 evolution of a microbial mutualism. *Proc. Natl. Acad. Sci.* **111**:14822–14827.
- 497 28. **Song HS, Renslow RS, Fredrickson JK, Lindemann SR.** 2015. Integrating ecological and  
498 engineering concepts of resilience in microbial communities. *Front. Microbiol.* **6**:1–7.
- 499 29. **Turkarslan S, Raman A V, Thompson AW, Arens CE, Gillespie MA, von Netzer F,**  
500 **Hillesland KL, Stolyar S, López García de Lomana A, Reiss DJ, Gorman Lewis D, Zane**  
501 **GM, Ranish JA, Wall JD, Stahl DA, Baliga NS.** 2017. Mechanism for microbial population  
502 collapse in a fluctuating resource environment. *Mol. Syst. Biol.* **13**:919.
- 503 30. **Thompson AW, Turkarslan S, Arens CE, López García de Lomana A, Raman A V., Stahl**  
504 **DA, Baliga NS.** 2017. Robustness of a model microbial community emerges from population  
505 structure among single cells of a clonal population. *Environ. Microbiol.* **19**:3059–3069.
- 506 31. **Kjelleberg S, Albertson N, Flardh K, Holmquist L, Jouper-Jaan A, Marouga R, Ostling J,**  
507 **Svenblad B, Weichart D.** 1993. How do non-differentiating bacteria adapt to starvation? *Antonie*  
508 *Van Leeuwenhoek* **63**:333–341.
- 509 32. **Shimizu K.** 2013. Regulation Systems of Bacteria such as *Escherichia coli* in Response to

- 510 Nutrient Limitation and Environmental Stresses. *Metabolites* **4**:1–35.
- 511 33. **Barbara S, Resources N, Collins F.** 2007. Microbial Stress-Response Physiology and Its  
512 Implications **88**:1386–1394.
- 513 34. **Roszak DB, Colwell RR.** 1987. Survival strategies of bacteria in the natural environment.  
514 *Microbiol. Rev.* **51**:365–379.
- 515 35. **Jørgensen BB, Marshall IPG.** 2016. Slow Microbial Life in the Seabed. *Ann. Rev. Mar. Sci.*  
516 **8**:311–332.
- 517 36. **Bergkessel M, Basta DW, Newman DK.** 2016. The physiology of growth arrest: uniting  
518 molecular and environmental microbiology. *Nat. Rev. Microbiol.* **14**:549–562.
- 519 37. **Lennon JT, Jones SE.** 2011. Microbial seed banks: The ecological and evolutionary implications  
520 of dormancy. *Nat. Rev. Microbiol.* **9**:119–130.
- 521 38. **Wanner U, Egli T.** 1990. Dynamics of microbial growth and cell composition in batch culture.  
522 *FEMS Microbiol. Rev.* **6**:19–43.
- 523 39. **Fritts RK, LaSarre B, Stoner AM, Posto AL, Mckinlay JB.** 2017. A Rhizobiales-specific  
524 unipolar polysaccharide adhesin contributes to *Rhodopseudomonas palustris* biofilm formation  
525 across diverse photoheterotrophic conditions **83**:1–14.
- 526 40. **Kim M-K, Harwood CS.** 1991. Regulation of benzoate-CoA ligase in *Rhodopseudomonas*  
527 *palustris*. *FEMS Microbiol. Lett.* **83**:199–203.
- 528 41. **Thomason LC, Costantino N, Court DL.** 2007. *E. coli* Genome Manipulation by P1  
529 Transduction. *Curr. Protoc. Mol. Biol.* 1.17.1-1.17.8.
- 530 42. **McKinlay JB, Zeikus JG, Vieille C.** 2005. Insights into *Actinobacillus succinogenes*  
531 Fermentative Metabolism in a Chemically Defined Growth Medium Insights into *Actinobacillus*  
532 *succinogenes* Fermentative Metabolism in a Chemically Defined Growth Medium. *Appl Env.*  
533 *Microbiol* **71**:6651–6656.
- 534 43. **Hayashi K, Morooka N, Yamamoto Y, Fujita K, Isono K, Choi S, Ohtsubo E, Baba T,**  
535 **Wanner BL, Mori H, Horiuchi T.** 2006. Highly accurate genome sequences of *Escherichia coli*

536 K-12 strains MG1655 and W3110. *Mol. Syst. Biol.* **2**:2006.0007.

537 44. **Larimer FW, Chain P, Hauser L, Lamerdin J, Malfatti S, Do L, Land ML, Pelletier D a,**  
538 **Beatty JT, Lang AS, Tabita FR, Gibson JL, Hanson TE, Bobst C, Torres JLTY, Peres C,**  
539 **Harrison FH, Gibson J, Harwood CS.** 2004. Complete genome sequence of the metabolically  
540 versatile photosynthetic bacterium *Rhodospseudomonas palustris*. *Nat. Biotechnol.* **22**:55–61.

541 45. **Trapnell C, Roberts A, Goff L, Pertea G, Kim D, Kelley DR, Pimentel H, Salzberg SL, Rinn**  
542 **JL, Pachter L.** 2012. Differential gene and transcript expression analysis of RNA-seq  
543 experiments with TopHat and Cufflinks. *Nat. Protoc.* **7**:562–578.

544 46. **Kim D, Pertea G, Trapnell C, Pimentel H, Kelley R, Salzberg SL.** 2013. TopHat2: accurate  
545 alignment of transcriptomes in the presence of insertions, deletions and gene fusions. *Genome*  
546 *Biol.* **14**:R36.

547 47. **Langmead B, Salzberg SL.** 2012. Fast gapped-read alignment with Bowtie 2. *Nat. Methods*  
548 **9**:357–9.

549 48. **Trapnell C, Williams BA, Pertea G, Mortazavi A, Kwan G, van Baren MJ, Salzberg SL,**  
550 **Wold BJ, Pachter L.** 2010. Transcript assembly and quantification by RNA-Seq reveals  
551 unannotated transcripts and isoform switching during cell differentiation. *Nat. Biotechnol.* **28**:511–  
552 515.

553 49. **The UniProt Consortium.** 2017. UniProt: The universal protein knowledgebase. *Nucleic Acids*  
554 *Res.* **45**:D158–D169.

555 50. **Kitagawa M, Ara T, Arifuzzaman M, Ioka-Nakamichi T, Inamoto E, Toyonaga H, Mori H.**  
556 2005. Complete set of ORF clones of *Escherichia coli* ASKA library (A complete set of *E. coli* K-  
557 12 ORF archive): unique resources for biological research. *DNA Res.* **12**:291–299.

558 51. **Blattner F, Plunkett G I, Bloch C, Perna N, Burland V, Riley M, Collado-Vides J, Glasner J,**  
559 **Rode C, Mayhew G, Gregor J, Davis N, Kirkpatrick H, Goeden M, Rose D, Mau B, Shao Y.**  
560 1997. The Complete Genome Sequence of *Escherichia coli* K-12. *Science (80-. ).* **277****1613**:1453–  
561 1462.

562 52. **Baba T, Ara T, Hasegawa M, Takai Y, Okumura Y, Baba M, Datsenko K a, Tomita M,**  
563 **Wanner BL, Mori H.** 2006. Construction of Escherichia coli K-12 in-frame, single-gene  
564 knockout mutants: the Keio collection. Mol. Syst. Biol. **2**:2006.0008.  
565

566 **Figure Legends**567 **Table 1. Selected differentially expressed transcripts in cocultures of *E. coli* and *R. palustris* compared to monocultures**

Species	Gene symbol	Gene description	<i>Rp</i> Nx + <i>Ec</i> WT		<i>Rp</i> NxΔAmtB + <i>Ec</i> WT		<i>Rp</i> ΔAmtB + <i>Ec</i> WT	
			Fold change <sup>c</sup>	FDR adjusted P-value	Fold change	FDR adjusted P-value	Fold change	FDR adjusted P-value
<i>E. coli</i>	rutA <sup>b</sup>	Pyrimidine monooxygenase	114.5 ± 0.0	0.09	108.0 ± 0.0	0.09	118.0 ± 0.1	0.09
	rutC <sup>b</sup>	Aminoacrylate peracid reductase	60.7 ± 0.1	0.01	58.0 ± 0.1	0.01	60.9 ± 0.1	0.01
	ddpX <sup>ab</sup>	D-ala dipeptidase	58.3 ± 0.1	0.01	59.9 ± 0.1	0.01	50.1 ± 0.0	0.01
	rutD <sup>b</sup>	Aminoacrylate hydrolase	56.9 ± 0.0	0.01	52.9 ± 0.1	0.01	56.6 ± 0.1	0.01
	rutE <sup>b</sup>	Malonic semialdehyde	48.8 ± 0.1	0.01	44.4 ± 0.1	0.01	48.2 ± 0.1	0.01
	rutF <sup>b</sup>	FMN reductase	45.2 ± 0.1	0.01	40.3 ± 0.1	0.01	45.5 ± 0.1	0.01
	patA <sup>ab</sup>	Putrescine aminotransferase	36.3 ± 0.1	0.01	33.6 ± 0.1	0.01	34.4 ± 0.0	0.01
	argT <sup>ab</sup>	Lysine/arginine/ornithine binding protein	35.1 ± 0.3	0.01	38.9 ± 0.3	0.01	35.3 ± 0.3	0.01
	rutG <sup>b</sup>	FMN reductase	28.5 ± 0.0	0.01	26.9 ± 0.0	0.01	29.0 ± 0.1	0.01
	ddpA <sup>ab</sup>	Probably dipeptide binding periplasmid protein	23.7 ± 0.0	0.01	26.8 ± 0.0	0.01	21.0 ± 0.0	0.01
	amtB <sup>ab</sup>	Ammonium transporter	21.3 ± 0.2	0.02	25.0 ± 0.2	0.01	24.1 ± 0.2	0.01
	metE	Methionine biosynthesis	-16.2 ± 0.1	0.03	23.6 ± 0.6	0.03	22.8 ± 0.5	0.02
	fimF	Fimbriae regulatory protein	-16.3 ± 0.0	0.01	18.4 ± 0.0	0.01	20.3 ± 0.1	0.01
	tar	Methyl-accepting chemotaxis protein II	-16.3 ± 0.2	0.01	15.8 ± 0.2	0.02	15.4 ± 0.2	0.01
	purL <sup>a</sup>	Purine biosynthesis	-16.8 ± 0.0	0.03	20.4 ± 0.1	0.02	18.8 ± 0.0	0.02
	flgD	Flagellar basal body rod modification protein	-17.1 ± 0.1	0.02	16.9 ± 0.0	0.01	17.4 ± 0.1	0.01
	ilvL <sup>a</sup>	Isoleucine biosynthesis	-17.4 ± 0.7	0.02	14.9 ± 0.4	0.02	14.2 ± 0.5	0.02
	pgaB	Glucosamine deacetylase	-17.9 ± 0.0	0.02	18.8 ± 0.0	0.03	17.3 ± 0.0	0.04
	ilvC <sup>a</sup>	Isoleucine biosynthesis	-18.0 ± 0.2	0.03	17.1 ± 0.2	0.04	17.6 ± 0.2	0.03
	metK	Methionine biosynthesis	-19.2 ± 0.1	0.03	17.5 ± 0.1	0.03	17.4 ± 0.1	0.04
	tap	Methyl-accepting chemotaxis protein IV	-19.7 ± 0.3	0.01	22.0 ± 0.2	0.01	22.1 ± 0.2	0.01
	flgC	Flagellar basal body	-20.1 ± 0.1	0.05				
	purK <sup>a</sup>	Purine biosynthesis	-20.7 ± 0.1	0.03	25.1 ± 0.1	0.01	21.02 ± 0.05	0.03
	metA	Methionine biosynthesis	-21.0 ± 0.1	0.02	20.6 ± 0.1	0.02	20.8 ± 0.2	0.02
	ilvG <sup>a</sup>	Isoleucine biosynthesis	-22.1 ± 0.1	0.01	19.3 ± 0.1	0.03	22.14 ± 0.07	0.01
	metF	Methionine biosynthesis	-23.3 ± 0.1	0.01	22.5 ± 0.1	0.01	17.62 ± 0.38	0.03
nadB	Aspartate oxidase	-24.3 ± 0.0	0.08	29.1 ± 0.1	0.05	23.74 ± 0.01	0.07	
<i>R. palustris</i>	RPA1206 <sup>a</sup>	Aldehyde dehydrogenase	36.0 ± 0.9	0.02			62.4 ± 0.4	0.01
	RPA1205 <sup>a</sup>	Putative alcohol dehydrogenase	32.8 ± 0.5	0.02			28.6 ± 0.4	0.01
	RPA0538	Putative porin	31.6 ± 2.3	0.03				
	RPA1009 <sup>a</sup>	Possible cytochrome P450	10.4 ± 0.8	0.03				
	RPA3101 <sup>a</sup>	Unknown	9.4 ± 0.3	0.03			10.3 ± 0.3	0.04
	RPA4045 <sup>a</sup>	Putative aa ABC transport	8.8 ± 0.4	0.02				
	RPA3100	Unknown	7.8 ± 0.2	0.02				
	RPA1010	Beta-lactamase-like	7.7 ± 0.4	0.04				
	RPA4020 <sup>a</sup>	Putative aa ABC transport permease	7.7 ± 0.2	0.02				
	RPA1204	Unknown	7.4 ± 0.1	0.02			7.4 ± 0.1	0.03
	RPA2376	Unknown	-6.9 ± 0.1	0.04	15.4 ± 0.2	0.04	9.0 ± 0.2	0.03
	RPA2142	Putative fatty acid CoA ligase	-7.3 ± 0.1	0.03				
	RPA2377	Unknown	-8.4 ± 0.2	0.02	16.4 ± 0.6	0.05	7.3 ± 0.1	0.02
	RPA2379	Probable acetyltransferase	-8.5 ± 0.3	0.02				



RPA2390	Possible Rhizobactin siderophore biosynthesis	-9.6 ± 0.2	0.06	22.8 ± 0.2	0.05	16.8 ± 0.5	0.03
RPA1260 <sup>a</sup>	Universal stress protein	-10.5 ± 0.0	0.02			7.2 ± 0.0	0.07
RPA2380	Possible tonB dep iron siderophore	-11.4 ± 0.6	0.03	17.1 ± 0.1	0.06	18.4 ± 0.2	0.01
RPA1259	Putative cation-transporting P-type ATPase	-11.6 ± 0.4	0.02			10.6 ± 0.0	0.06
RPA2378 <sup>a</sup>	Putative TonB-dep receptor	-13.1 ± 0.1	0.03	24.1 ± 0.3	0.06	17.5 ± 0.3	0.02

568 Genes shown in table were directly or indirectly mentioned in the text. For a full list of differentially-expressed genes, see Supplementary Data.

569 <sup>a</sup> Genes were also identified as differentially expressed proteins in coculture (Table 2)

570 <sup>b</sup> Gene is transcriptionally activated by *E. coli* NtrC during nitrogen limitation

571 <sup>c</sup> Fold-change values represent mean ± SD. Positive values indicate gene was upregulated in coculture. Negative values indicate gene was  
572 downregulated in coculture. Initial cutoff was set to a log<sub>2</sub> value of 2 in at least 2 of 3 biological replicates. For a complete list of all differentially  
573 regulated transcripts, refer to supplementary data. Differential expression was determined with the Cufflinks tool cuffdiff (v.2.2.0) (45)

574 **Table 2. Selected differentially expressed proteins in cocultures of *E. coli* and *R. palustris* compared**  
575 **to monocultures**

Species	Gene Symbol	Gene Description	Rp Nx + Ec WT	Rp NxΔAmtB + Ec WT
			Normalized Relative Protein Intensity <sup>c</sup>	Normalized Rela Protein Intensit
<i>E. coli</i>	argT <sup>ab</sup>	Lysine/arginine/ornithine binding protein	10.9	11.1
	ddpA <sup>ab</sup>	D-ala dipeptide permease	5.8	7.2
	gss	Bifunctional glutathionylspermidine synthetase/amidase	4.5	4.7
	tktB	Transketolase	4.1	5.5
	potF <sup>ab</sup>	Putrescine-binding periplasmic protein	3.8	4.2
	modA	Molybdate-binding periplasmic protein	3.8	4.0
	gabD <sup>ab</sup>	Succinate-semialdehyde dehydrogenase	3.7	4.8
	dapB	4-hydroxy-tetrahydrodipicolinate reductase	3.6	2.8
	talA	Transaldolase A	3.6	4.2
	amtB <sup>ab</sup>	NH4 <sup>+</sup> Transporter	3.5	3.5
	asnS	Asparagine biosynthesis	-2.1	-1.9
	serA	Serine biosynthesis	-2.1	-2.5
	secE	Protein translocase subunit	-2.1	-1.8
	glf	LPS biosynthesis	-2.1	-1.9
	yjiM	Putative dehydratase	-2.2	-1.9
	sstT	Serine/threonine transporter	-2.2	-2.4
	rmlA1	Carbohydrate biosynthesis	-2.3	-2.1
	ompF	Outer membrane protein	-2.3	-2.3
	ribE	Riboflavin biosynthesis	-2.3	-1.7
	secY	Protein translocase subunit	-2.6	-2.0
glyA	Glycine biosynthesis	-3.2	-3.0	
purE <sup>a</sup>	Purine biosynthesis	-3.3	-3.6	
yqjI	Transcriptional regulator	-3.6	-3.0	
asnA	Aspartate-ammonia ligase	-6.4	-3.8	
<i>R. palustris</i>	RPA1206 <sup>a</sup>	Aldehyde dehydrogenase	10.0	
	RPA1205 <sup>a</sup>	Putative alcohol dehydrogenase	7.8	1.2
	RPA3101 <sup>a</sup>	Unknown	7.1	1.5
	RPA3093	ABC transporter urea/short-chain binding protein	4.8	1.6
	RPA3297	ABC transporter urea/short-chain binding protein	4.7	1.5
	RPA4019	Putative aa ABC transporter system substrate-binding protein	3.9	1.4
	RPA4045 <sup>a</sup>	Putative aa ABC transport	3.3	1.4
	RPA1009 <sup>a</sup>	Possible cytochrome P450	3.2	1.3
	RPA1748	Putative branched-chain amino acid transport system substrate-binding protein	-2.1	-1.4
	RPA2378 <sup>a</sup>	Putative tonB-dependent receptor protein	-2.1	-1.2
	RPA2124	TonB dependent iron siderophore receptor	-2.3	-1.5
	RPA1260 <sup>a</sup>	Universal stress protein	-2.5	-1.5
	RPA2050	Unknown	-2.7	-1.6
	RPA3669	Putative ABC transporter periplasmic solute-binding protein precursor	-2.8	-1.1
	RPA2120	Periplasmic binding protein	-6.0	-1.6

576  
577 Proteins shown in table were directly or indirectly mentioned in the text. For a full list of differentially-  
578 expressed proteins, see Supplementary Data.

579 <sup>a</sup> Genes were also identified as differentially expressed transcripts in coculture (Table 1)

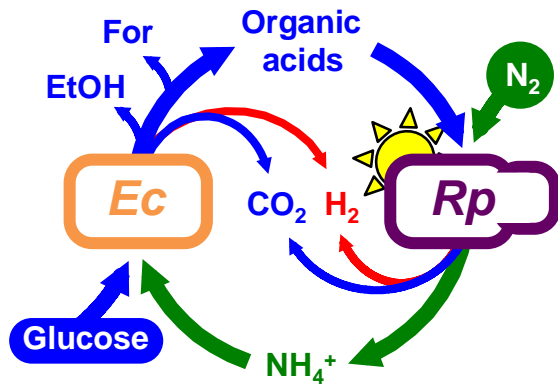
580 <sup>b</sup> Gene is transcriptionally activated by *E. coli* NtrC

581 Values represent mean normalized relative protein intensity for either two<sup>c</sup> or one<sup>d</sup> biological replicate.

582 Positive values indicate gene was upregulated in coculture. Negative values indicate gene was

583 downregulated in coculture.

584



585

586 **FIG 1. Bidirectional cross-feeding of carbon and nitrogen in an anaerobic bacterial mutualism**

587 **between fermentative *Escherichia coli* (*Ec*) and phototrophic *Rhodospseudomonas palustris* (*Rp*).** *E.*

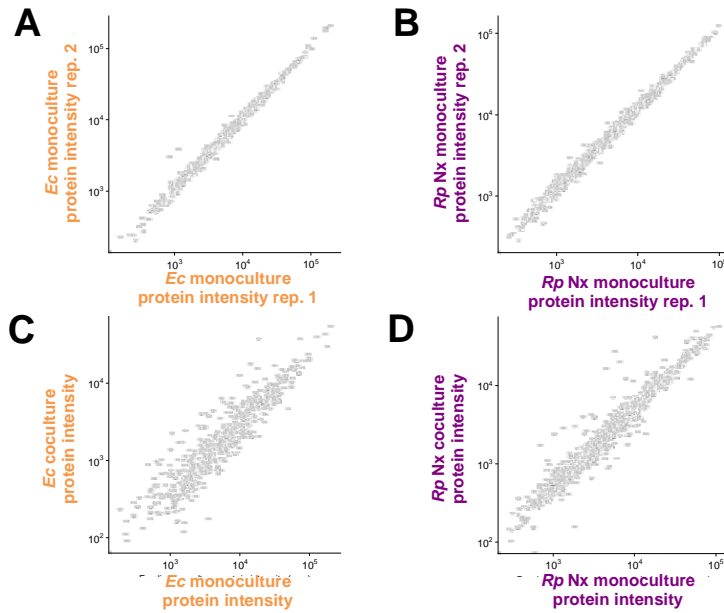
588 *coli* anaerobically ferments glucose into excreted organic acids that *R. palustris* Nx consumes (acetate,

589 lactate and succinate) and other products that *R. palustris* Nx does not consume (formate (For) and

590 ethanol (EtOH)). In return, *R. palustris* Nx constitutively fixes N<sub>2</sub> gas and excretes NH<sub>4</sub><sup>+</sup>, supplying *E.*

591 *coli* with essential nitrogen. *R. palustris* Nx grows photoheterotrophically wherein organic compounds are

592 used for carbon and electrons and light is used for energy.



593

594

**FIG 2. Coculturing results in altered protein expression patterns in both species, with more**

595

**differences in WT *E. coli* compared to *R. palustris* Nx. Protein expression (estimated by LC-**

596

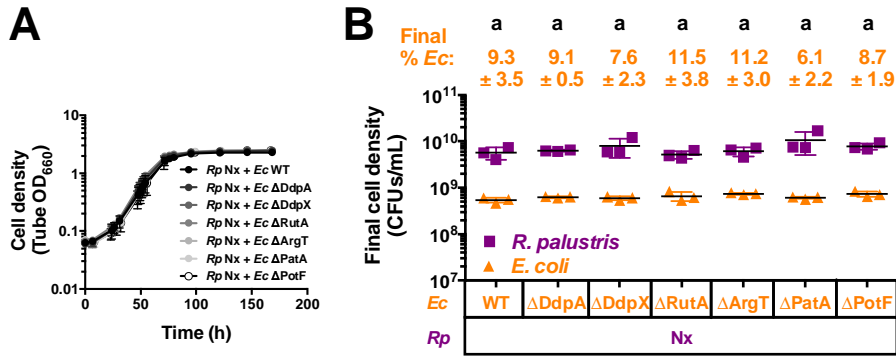
**MS/MS intensity) of wild-type *E. coli* (left, **A,C**) and *R. palustris* Nx (right, **B,D**) comparing**

597

**protein expression patterns between monoculture biological replicates (rep. 1 versus rep. 2, **A,B**)**

598

**and monoculture (average over monoculture replicates) versus coculture (**C,D**).**



599

600 **FIG 3. Single deletions of upregulated *E. coli* genes do not impair mutualistic growth with *R.***

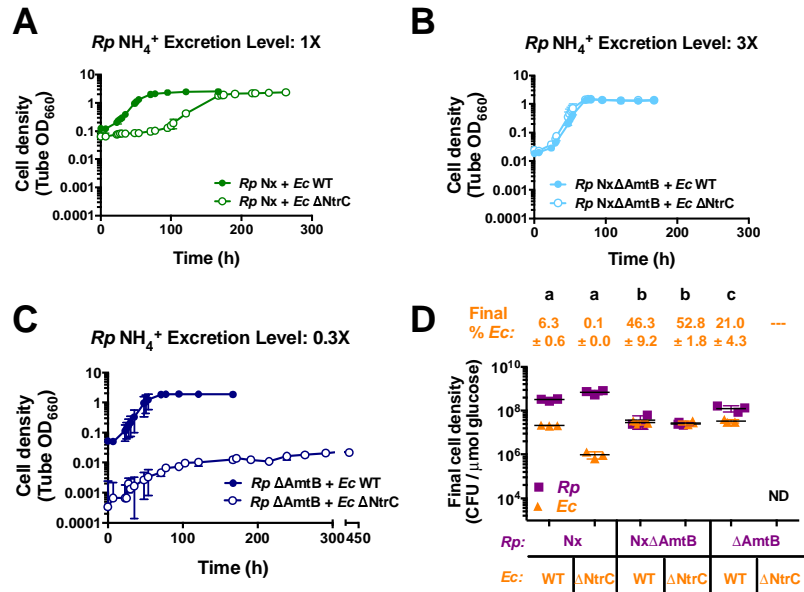
601 ***palustris* Nx.** Growth curves (A) and final cell densities (B) from cocultures pairing *E. coli* (*Ec*) mutants

602 with deletions in highly upregulated genes with *R. palustris* (*Rp*) Nx. Final cell densities were taken at the

603 final time point indicated in (A). Cocultures were started with a 1% inoculum of stationary starter

604 cocultures grown from single colonies. Error bars indicate SD, n=3. Different letters indicate statistical

605 differences,  $p < 0.05$ , determined by one-way ANOVA with Tukey's multiple comparisons posttest.



606

607 **FIG 4. *R. palustris* NH<sub>4</sub><sup>+</sup> excretion level affects growth and population trends in cocultures with *E.***

608 ***coli* NtrC.** Growth curves (A,B,C) and final cell densities normalized to glucose consumption (D) from

609 cocultures pairing WT *E. coli* (*Ec*) (filled circles) or ΔNtrC (open circles) with different *R. palustris* (*Rp*)

610 strains that have different NH<sub>4</sub><sup>+</sup> excretion levels. Final cell densities were taken at the final time point

611 indicated in the respective growth curve, except for cocultures pairing *R. palustris* ΔAmtB with *E. coli*

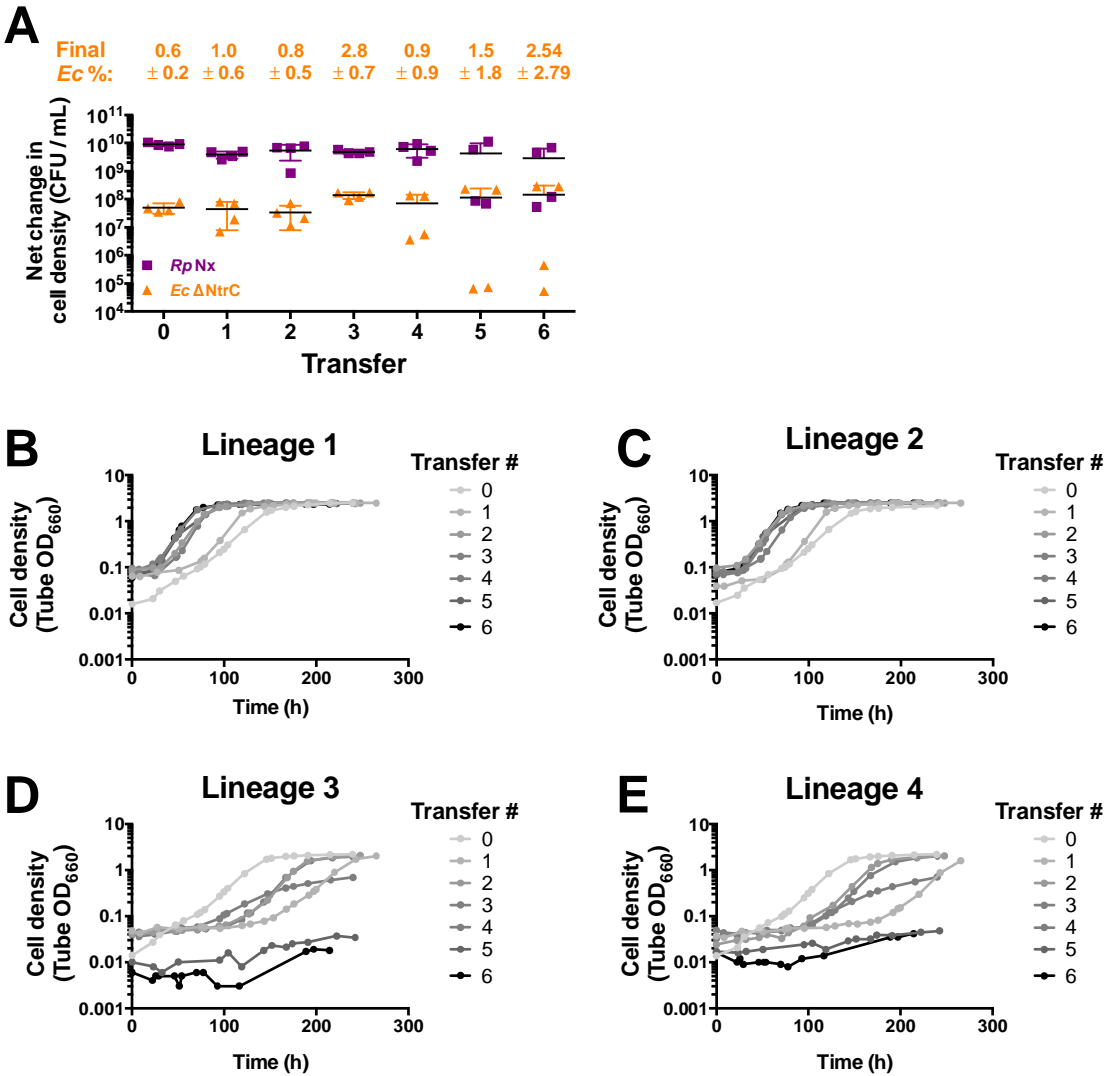
612 ΔNtrC which were sampled at 260 h. Cell densities were normalized to glucose consumed to account for

613 incomplete glucose consumption in cocultures containing *E. coli* ΔNtrC. Cocultures were started with a

614 1% inoculum of stationary starter cocultures grown from single colonies. Error bars indicate SD, n=3.

615 Different letters indicate statistical differences,  $p < 0.05$ , determined by one-way ANOVA with Tukey's

616 multiple comparisons posttest. ND, not determined.



617

618

**FIG 5. Lack of *E. coli* NtrC results in variable coculture growth trends across serial transfers.** Net

619

changes in cell densities (A) and replicate growth curves (B-E) of cocultures pairing *E. coli* (*Ec*)  $\Delta$ NtrC

620

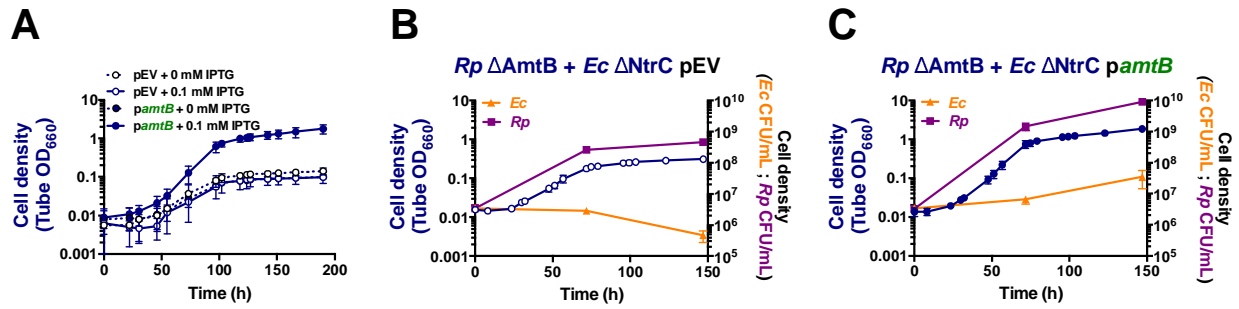
with *R. palustris* (*Rp*) Nx across serial transfers. Cocultures were initially inoculated (Transfer 0) at a 1:1

621

starting species ratios based on CFUs/mL from *R. palustris* and *E. coli* monocultures. A 1% inoculum

622

was used for each serial transfer. Transfers were performed every 10 d. Error bars indicate SD, n=4.



623

624 **FIG 6. Ectopic expression of *amtB* in *E. coli*  $\Delta$ NtrC permits mutualistic growth with *R. palustris***

625  **$\Delta$ AmtB.** Growth curves (A-C) and cell densities for each species (B,C) from cocultures pairing *R.*

626 *palustris* (*Rp*)  $\Delta$ AmtB with *E. coli* (*Ec*)  $\Delta$ NtrC harboring a plasmid encoding an IPTG-inducible copy of

627 *amtB* (*pamtB*, filled circles) or an empty vector (*pEV*, open circles). To maintain plasmids, all cocultures

628 were supplemented with 5  $\mu$ g/ml chloramphenicol, which is otherwise lethal to *E. coli* but not to *R.*

629 *palustris* (Fig. S6). Cocultures were inoculated with a single colony of each species (A) or at a 1:1

630 starting species ratio based on equivalent CFUs/mL from starter *R. palustris* and *E. coli* monocultures

631 (B,C). 0.1 mM IPTG was added to the cocultures at the initial time point. Error bars indicate SD, n=3.



## 632 Supplemental

## 633 Table S1. Strains and plasmids

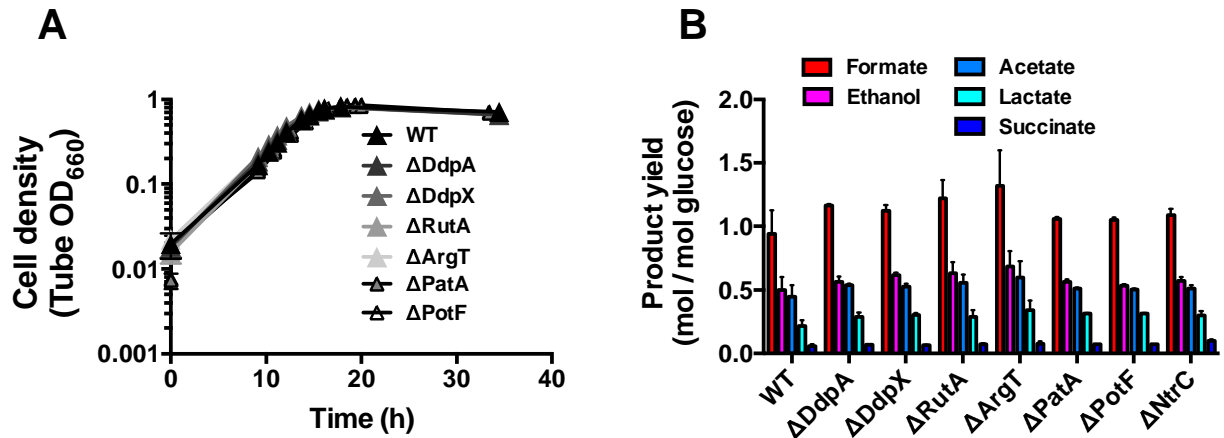
Strain or plasmid	Description or Sequence (5'-3'); <u>Designation</u>	Source or Purpose
<b><i>R. palustris</i> strains</b>		
CGA009	Wild-type strain; spontaneous Cm <sup>R</sup> derivative of CGA001	(44)
CGA4005	CGA009 $\Delta hupS \Delta uppE nifA^*$ ; <u>Nx</u>	(10)
CGA4021	CGA4005 $\Delta amtB1 \Delta amtB2$ ; <u>Nx</u> $\Delta AmtB$	(10)
CGA4026	CGA009 $\Delta hupS \Delta uppE \Delta amtB1 \Delta amtB2$ ; <u><math>\Delta AmtB</math></u>	(12)
<b><i>E. coli</i> strains</b>		
MG1655	Wild-type K12 strain; <u>WT</u>	(51)
K-12 JW1483	Keio collection $\Delta ddpX::Km$	(52)
K-12 JW5240	Keio collection $\Delta ddpA::Km$	(52)
K-12 JW0997	Keio collection $\Delta rutA::Km$	(52)
K-12 JW2307	Keio collection $\Delta argT::Km$	(52)
K-12 JW5510	Keio collection $\Delta patA::Km$	(52)
K-12 JW0838	Keio collection $\Delta potF::Km$	(52)
K-12 JW3840	Keio collection $\Delta ntrC::Km$	(52)
K-12 pCA24N (pASKA)	ASKA collection pCA24N	(50)
MG1655 pCA24N -GFP	ASKA collection pCA24N with gfp removed using NotI digest	This study
K-12 JW0441-AM pASKAamtB	ASKA collection pCA24N-N-His-amtB (gfp minus)	(50)
MG1655 $\Delta DdpX$	MG1655 $\Delta ddpX::Km$ ; <u><math>\Delta DdpX</math></u>	This study
MG1655 $\Delta DdpA$	MG1655 $\Delta ddpA::Km$ ; <u><math>\Delta DdpA</math></u>	This study
MG1655 $\Delta RutA$	MG1655 $\Delta rutA::Km$ ; <u><math>\Delta RutA</math></u>	This study
MG1655 $\Delta ArgT$	MG1655 $\Delta argT::Km$ ; <u><math>\Delta ArgT</math></u>	This study
MG1655 $\Delta PatA$	MG1655 $\Delta patA::Km$ ; <u><math>\Delta PatA</math></u>	This study
MG1655 $\Delta PotF$	MG1655 $\Delta potF::Km$ ; <u><math>\Delta PotF</math></u>	This study
MG1655 $\Delta NtrC$	MG1655 $\Delta ntrC::Km$ ; <u><math>\Delta NtrC</math></u>	This study
MG1655 pEV	MG1655 pCA24N; <u>WT pEV</u>	This study
MG1655 $\Delta NtrC$ pEC	MG1655 $\Delta ntrC::Km$ pCA24N; <u><math>\Delta NtrC</math> pEV</u>	This study
MG1655 <i>pamtB</i>	MG1655 pCA24N-N-His- <i>amtB</i> +; <u>WT <i>pamtB</i></u>	This study
MG1655 $\Delta NtrC$ <i>pamtB</i>	MG1655 $\Delta ntrC::Km$ pCA24N-N-His- <i>amtB</i> +; <u><math>\Delta NtrC</math> <i>pamtB</i></u>	This study
<b>Plasmids</b>		
pCA24N	Cm <sup>R</sup> ; ASKA collection empty vector with IPTG-inducible promoter	(50)
pCA24N- <i>amtB</i> +	Cm <sup>R</sup> ; ASKA collection vector with IPTG-inducible promoter in front of N-terminal His-tagged <i>amtB</i> gene	(50)
<b>Primers</b>		

ALM47	cggaagcgcagcaattttgt	<i>ddpX</i> upstream flanking region ( <i>E. coli</i> )
ALM48	gagcaatgtgggacgaaacg	<i>ddpX</i> downstream flanking region ( <i>E. coli</i> )
ALM45	atatcccctggcacacagc	<i>ddpA</i> upstream flanking region ( <i>E. coli</i> )
ALM46	ccagcagcgttggcgtaaata	<i>ddpX</i> downstream flanking region ( <i>E. coli</i> )
ALM51	ccgcttgcaacaagcc	<i>rutA</i> upstream flanking region ( <i>E. coli</i> )
ALM52	atcagcgactttgctgc	<i>rutA</i> downstream flanking region ( <i>E. coli</i> )
ALM49	gcaaacacacacacaatacacaac	<i>argT</i> upstream flanking region ( <i>E. coli</i> )
ALM50	ccatcaggtacagcttcca	<i>argT</i> downstream flanking region ( <i>E. coli</i> )
ALM53	tgaaagcgtgctgtaacgc	<i>patA</i> upstream flanking region ( <i>E. coli</i> )
ALM54	atcccgatatttcgcatcg	<i>patA</i> downstream flanking region ( <i>E. coli</i> )
ALM55	ctggccgggagaaagtct	<i>potF</i> upstream flanking region ( <i>E. coli</i> )
ALM56	ttacgggttttcgcctgc	<i>potF</i> downstream flanking region ( <i>E. coli</i> )
MO 7	caatctttacacacaagctgtgaatc	<i>ntrC</i> upstream flanking region ( <i>E. coli</i> )
MO 8	cctgcctatcaggaataaaagg	<i>ntrC</i> downstream flanking region ( <i>E. coli</i> )
pCA24N.for	gataacaatttcacacagaattcattaagag	ASKA pCA24N upstream into IPTG-inducible promoter upstream of cloned gene
pCA24N.rev	cccattaacatcaccatctaattcaac	ASKA pCA24N downstream into IPTG-inducible promoter upstream of cloned gene

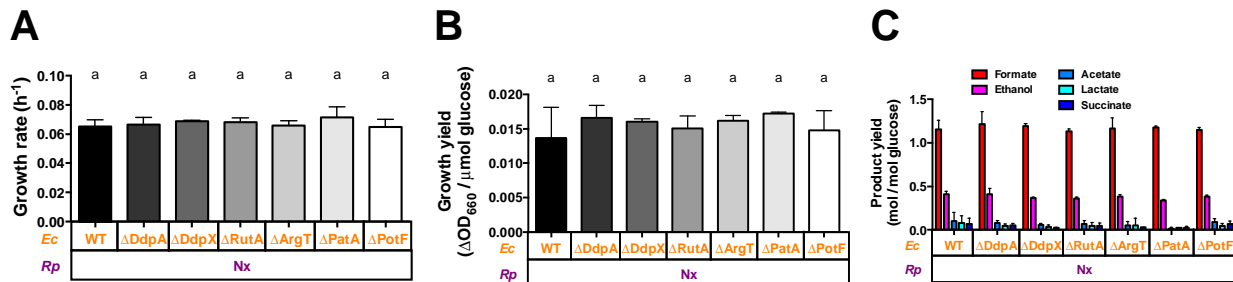
634

635

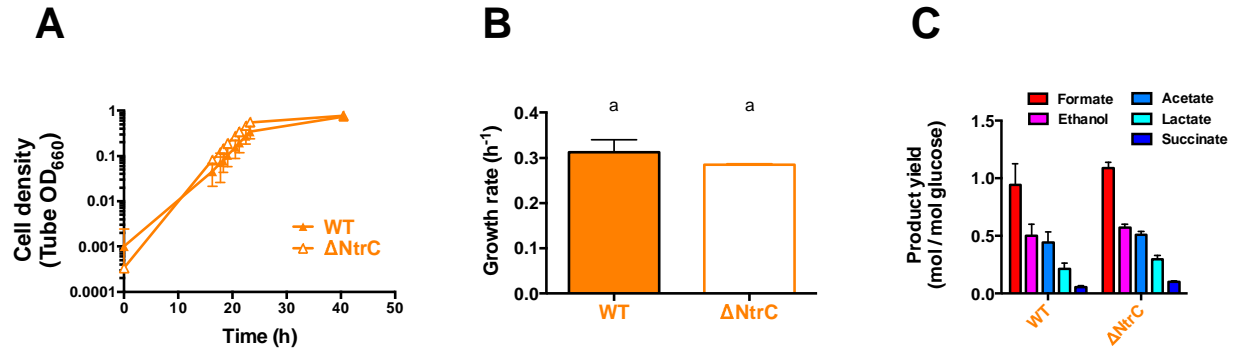
636



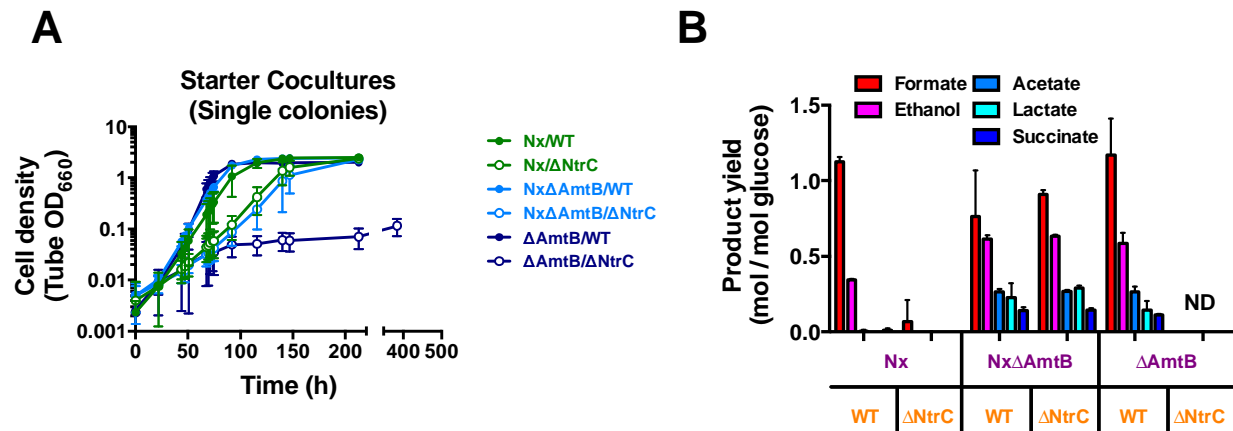
637  
 638 **FIG S1. Single deletions of *E. coli* genes that were upregulated in coculture no effect in monoculture**  
 639 **with 15 mM NH<sub>4</sub><sup>+</sup>.** Growth curves (A) and product yields (B) from *E. coli* monocultures grown with 15  
 640 mM NH<sub>4</sub>Cl. Product yields were taken in stationary phase. Error bars indicate SD, n=3.  
 641



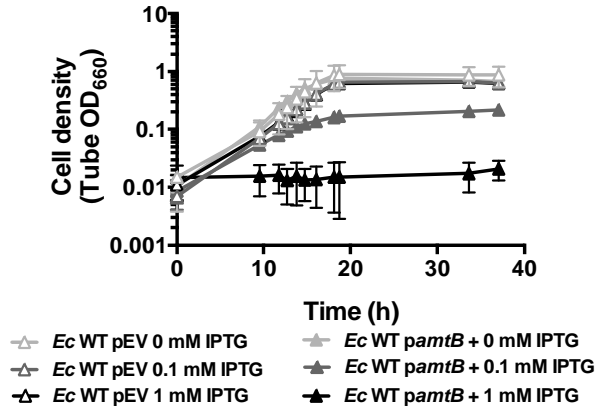
642  
 643 **FIG S2. Additional trends from cocultures pairing *R. palustris* Nx with *E. coli* single deletion**  
 644 **mutants.** Growth rates (A), growth yields (B), and product yields (C) after a one-week culturing period  
 645 from cocultures pairing *E. coli* mutants with deletions in highly upregulated genes with *R. palustris* Nx.  
 646 Growth and product yields were taken at the final time point indicated in Fig. 3A. Cocultures were started  
 647 with a 1% inoculum of stationary starter cocultures grown from single colonies. Error bars indicate SD,  
 648 n=3. Different letters indicate statistical differences, p < 0.05, determined by one-way ANOVA with  
 649 Tukey's multiple comparisons posttest.



650  
 651 **FIG S3. *E. coli*  $\Delta$ NtrC growth and metabolic trends are similar to those of WT *E. coli* in**  
 652 **monoculture with 15 mM  $\text{NH}_4^+$ .** Growth curves (A), growth rate (B) and product yields (C) from WT *E.*  
 653 *coli* (filled) or  $\Delta$ NtrC (open) monocultures grown with 15 mM  $\text{NH}_4\text{Cl}$ . Product yields were taken in  
 654 stationary phase. Error bars indicate SD, n=3.  
 655



656  
 657 **FIG S4. Additional trends from cocultures of *E. coli*  $\Delta$ NtrC paired with different *R. palustris***  
 658 **partners.** Growth curves of starter cocultures inoculated with single colonies of each species (A) and  
 659 product yields from test cocultures (B). Product yields were taken at the final time point indicated in the  
 660 respective growth curve in Fig. 4. Test cocultures were started with a 1% inoculum of stationary starter  
 661 cocultures. Error bars indicate SD, n=3. ND, not determined.



662

663 **FIG S5. Increased *amtB* expression is harmful to *E. coli* in monocultures with 15 mM NH<sub>4</sub><sup>+</sup>.** Growth

664 curves of WT *E. coli* monocultures harboring a plasmid encoding an IPTG-inducible copy of *amtB*

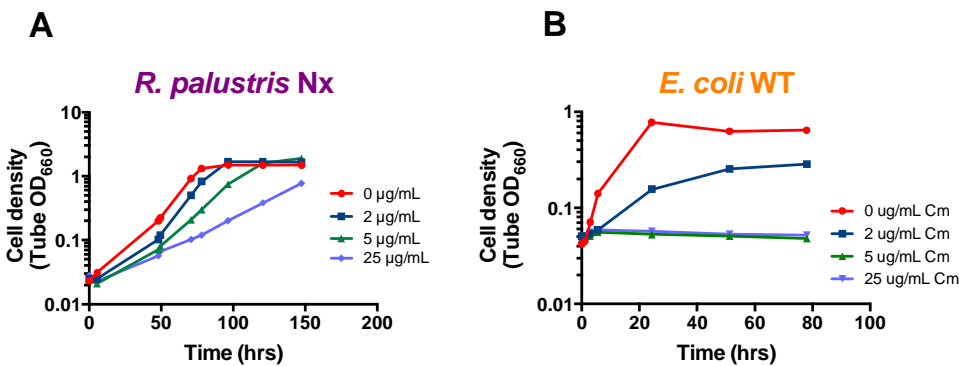
665 (*pamtB*, filled) or empty vector (pEV, open) and grown at different IPTG concentrations. All

666 monocultures were supplemented with 15 mM NH<sub>4</sub>Cl and 5 μg/ml chloramphenicol to maintain the

667 plasmid. Cultures were inoculated with a 1% inoculum from stationary monocultures grown in 0 mM

668 IPTG. After inoculation, IPTG was added to the indicated final concentration. Error bars indicate SD,

669 n=3. ND, not determined.



670

671 **FIG S6. Determination of a chloramphenicol concentration to maintain *pamtB* in *E. coli* without**

672 **harming *R. palustris*.** Representative growth curves of *R. palustris* Nx (A) and WT *E. coli* (B) at

673 different concentrations of chloramphenicol. All cultures were grown anaerobically in MDC with a 1%

674 inoculum from stationary monocultures. *R. palustris* Nx was provided 20 mM sodium acetate as a carbon

675 source with a 100% N<sub>2</sub> headspace for nitrogen. WT *E. coli* was provided 25 mM glucose, 10 mM cation

676 solution, and 15 mM NH<sub>4</sub>Cl.